35th International Workshop on Water Waves and Floating Bodies, 26-29 April 2020, Seoul, Korea

Vertical column in strong water wave events: runup, runup velocity and their scaling

John Grue and Bodgan Osyka
Mechanics Division, Department of Mathematics, University of Oslo, Oslo, Norway
email: johng@math.uio.no

1 Motivation

Offshore wind farm developments is a growing industry where the Dogger Bank project in the North Sea in Europe is a newcomer. The contract to Equinor and SSE Renewables concerns the construction of a total installed capacity of 3.6 GW. Vertical columns are placed on the sea floor where a water depth of 20 m - 35 m is typical. The waves may be strong, non-breaking or breaking. Questions include the wave characteristics, wave loads and runup along the columns.

This paper concerns wave runup, runup velocity and their scaling. Faltinsen et al. (2004) have noted that the description of wave runup is not state-of-the-art. Both horizontal and vertical loads should be considered. De Vos et al. (2007) and Lykke Andersen et al. (2011) have listed several reasons why runup on slender vertical cylinders caused by breaking and non-breaking waves are important. They performed experiments with slender cylinders using a random wave input at finite depth. Buchmann et al. (2000) employed a fully nonlinear time-domain boundary element model and a second-order time-domain boundary element model to investigate runup. The cylinder was bottom-mounted at intermediate depth with calculations for low wave slope and Froude number. Recently, Zhang and Teng (2017) calculated the runup on a vertical cylinder exposed to cnoidal waves in shallow water. We shall compare our measurements to existing results.

2 Experiments

We perform wave tank measurements of the runup on a vertical cylinder exposed to focusing waves. The runup is obtained by use of video recordings, with subsequent digitalization of the elevation at five different positions along the circumference of the cylinder. The runup velocity is obtained by a time derivative of the runup motion. The input wave conditions are strong. The waves are shallow or at intermediate depth with $kh \sim 0.65 - 1.8$. We also discuss briefly runup in deep water.

The experiments were performed in a 25 m long and 0.5 m wide wave tank in the Hydrodynamics Laboratory at the University of Oslo. A vertical cylinder of radius $R = 3$ cm was positioned 10.86 m from the wave maker and 10.23 m from an absorbing beach of length 3.51 m, at the opposite end of the tank. The water depth h was 0.25 m or 0.15 m giving depth to cylinder diameter ratios of 4.16 and 2.5, respectively. Focusing waves were generated using standard techniques. The elevation of the incoming waves was measured by ultra sound UltraLab ULS Advanced system. This combines one transmitting sensor and two receiving sensors operating at 250 Hz.

Runup on the cylinder was filmed using Photron's FASTCAM SA5 High-Speed Video System (www.photron.com). A frame rate of 500 fps was used, where the camera provides up to 7500 fps. The resolution is 1024 times 1000. The VLX2 LED Line Lightening (Gardasoft Vision) light source used in the recordings has maximum intensity of 2.3×10^6

Lux. The light intensity was controlled and adjusted using the Tera Term terminal software. We have obtained also the overturning moment on the cylinder (with respect to the bottom) using force transducers HBM (www.hbm.com), for illustrative purposes. The sensors and camera were mapped against each other using analog trigger circuitry (ATC). The ATC generated an internal trigger signal to initiate the acquisition (www.ni.com). This was monitored relative to the paddle motion. We thus obtained, at syncronized time, the input wave elevation, runup motion and overturning moment. The recordings were obtained long before any small reflections from the beach occurred at the position of the cylinder.

Ten focusing wave events were produced with a water depth of $h = 25$ cm and another six runs with $h = 15$ cm. The elevation was measured at the position of the cylinder with the cylinder absent. The crest height ($\eta_{0,m}$) and the trough-to-trough wave period (T_{TT}) were extracted. The wave frequency is estimated by $\omega = 2\pi/T_{TT}$, wavenumber by $\omega^2 = gk \tanh kh$ and a reference speed defined by $c^h_{ref} = g/\omega$.

3 Runup

Snapshot of the wave runup at maximum, in the strongest case, is shown in figure 1a. The runup is obtained at five positions along the cylinder contour (positions 1-5). In terms of the angle along the cylinder contour, position 1 is at the weather side at an angle of 0°, position 2 at 41.4°, position 3 at 60°, position 4 at 75.7°, and position 5 at 90°. The runup at each positions is obtained as function of time (figure 1b). A cubic polynomial least squares fit to the experimental recordings obtain the runup $Y_i(t)$ as a continuous and differentiable function. In the figure, time t_0 is defined at maximum runup. Maximum crest height of the input wave occurs at $\omega(t - t_0) = -0.847$ and maximum overturning moment at $\omega(t-t_0) = -0.820$ in this run. A time derivative obtains the runup velocity as presented by the symbols in figure 1c. The run-up velocity approximated by $[2g(Y_{i,max} - y)]^{1/2}$ is presented by the solid/dashed-dotted/dashed lines.

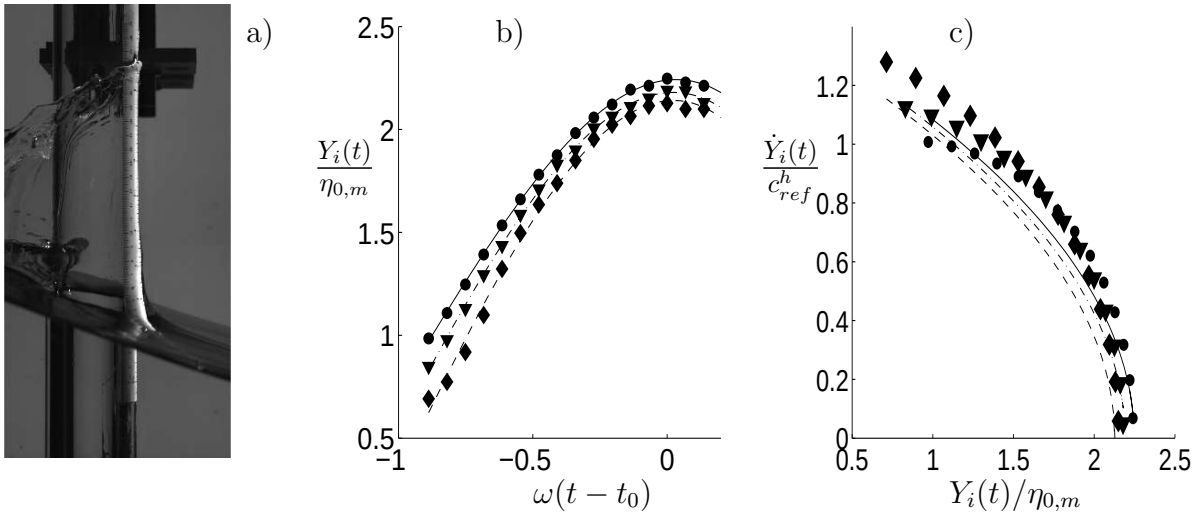

Figure 1: a) Video recording of runup. b) Discretized runup $Y_i(t)$ vs. time $\omega(t - t_0)$. c) Runup velocity $\dot{Y}_i(t)$ vs. $Y_i(t)$. Plot c) includes velocity estimates by $[2g(Y_{i,max} - y)]^{1/2}$ at 0° (——), 60° (− · −·), 90° (−−). Positions along the cylinder contour: 0° (front face, •, ——), 60° (▼, − · −·), 90° (⧫, −−). Wave moving from right to left. Non-breaking wave with $k\eta_{0.m} = 0.543$ and $kh = 1.37$. Wave breaks right behind the cylinder. Time t_0 at maximum runup.

We denote by $Ru_m = \max(Y_1(t))$ the maximum runup on the weather side. This is up to $Ru_m/\eta_{0,m} = 2.25$ at maximum. The experimental data of the runup of the 16 runs are rather scattered (figure 2a). Following De Vos et al. (2007) and Lykke Andersen et al. (2011) the runup may be connected to the (horizontal) orbital velocity at crest (u_m) by

$$Ru_m - \eta_{0,m} = (1/2)\, M\, u_m^2/g, \tag{1}$$

where M is a factor. This motivates for a scaling of the runup by

$$\widetilde{Ru}_m^{\,h} = [2g(Ru_m - \eta_{0,m})]^{1/2}/c_{ref}^h. \tag{2}$$

This function is plotted in figure 2b. In fact, all among the experimental data including both depth to cylinder diameter ratios cluster along one common straight line. The latter is obtained by a linear fit to the experimental points obtaining: $k\eta_{0,m} = 0.0635 + 0.473\widetilde{Ru}_m^{\,h}$. This relation obtains explicitly the maximum runup at finite water depth in terms of the wave slope $k\eta_{0,m}$ and $\tanh kh$.

For comparison to other work, De Vos et al. (2007) showed in one case the time series of the wave elevation and runup which otherwise was expressed in terms of statistical variables. The resulting nondimensional data for the random wave event and runup in their figure 15, become: ($kh = 0.84$, $k\eta_{0,m} = 0.28$, $Ru_m/\eta_{0,m} = 1.8$). This data point contibutes to the scatter in figure 2a where $Ru_m/\eta_{0,m}$ is plotted vs. $k\eta_{0,m}$. In figure 2b where $[2g(Ru_m - \eta_{0,m})]^{1/2}/c_{ref}^h$ is plotted vs. wave slope, the data point obtained from De Vos et al. fits rather well to the present measurements.

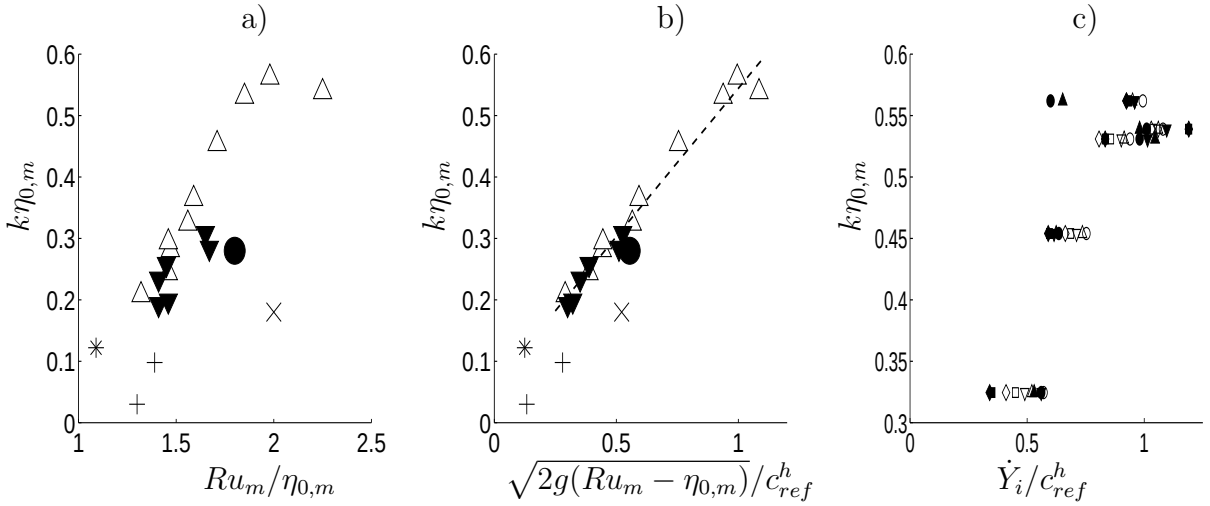

Figure 2: a) and b) Run-up maximum Ru_m at front face of the cylinder (at 0 degrees) vs. wave slope $k\eta_{0,m}$. $h/2R = 4.16$ (Δ), $h/2R = 2.5$ ($\blacktriangledown$). $k\eta_{0,m} = 0.0635 + 0.473\sqrt{2g(Ru_m - \eta_{0,m})}/c_{ref}^h$ (linear fit, $- - -$). Event in random waves by De Vos et al. (2007, figure 15) ($\bullet$); periodic waves by De Vos et al. (2007, figure 6) ($*$); periodic 2nd order theory ($\times$), $h/2R = 0.5$ (Buchmann et al., 2000, fig. 9A); cylinder with $h/2R = 1.2$ in cnoidal waves ($+$) (Zhang and Teng, 2017, fig. 13). c) Run-up velocity at $y = \eta_{0,m}$ vs. $k\eta_{0,m}$. Measured: black symbols; $[2g(Y_{i,m} - \eta_{0,m})]^{1/2}$ open symbols. 0° ($\bullet$ $\circ$); 41.4° ($\blacktriangle$, $\triangle$); 60° ($\blacktriangledown$, $\triangledown$); 75.7° ($\blacksquare$, $\square$); 90° ($\blacklozenge$, $\lozenge$).

For periodic waves, De Vos et al. (2007, figure 6) presented a time series of the elevation and runup obtaining: $kh = 1.02$, $kA = 0.12$, $Ru_m/A = 1.09$, where A denotes wave amplitude. The data produces $[2g(0.065-0.06)\text{m}]\omega/g = 0.125$ which fits well to the results in figure 2b. The runup is much greater on the wider cylinders as calculated by Buchmann et al. (2000) and Zhang and Teng (2017).

The runup velocity grows with increasing waveslope to a nondimensional maximum of 1.2 for the strongest wave where the runup is also at maximum and where $k\eta_{0,m} = 0.543$ (figure 2c). Note that the wave is non-breaking in this strongest event. The nondimensional runup velocity decays to a value slightly less than unity for an even stronger wave with $k\eta_{0,m} = 0.559$ which is also breaking. The results illustrate that wave breaking reduces both runup height and runup velocity. The approximation of the runup velocity by $v(y) = [2g(Y_{i,m} - y)]^{1/2}$ underpredicts the measurement by approximately 10 per cent in the strongest case. This simplification provides a useful estimate of runup velocity.

The present measurements may be connected to field scale. By using a water depth of $h = 35$ m which is relevant for the conditions at the wind farm development at Dogger Bank in the North Sea, and a corresponding cylinder diameter of 8.4 m, we obtain from the parameters in the strongest runs:

non-breaking $\quad \eta_{0,m} = 12.9$ m $\quad Ru_m = 28.9$ m $\quad g/\omega = 14.5$ ms^{-1} $\quad \max \dot{Y}_i = 17.8$ ms^{-1},
breaking $\quad \eta_{0,m} = 13.3$ m $\quad Ru_m = 26.8$ m $\quad g/\omega = 14.8$ ms^{-1} $\quad \max \dot{Y}_i = 14$ ms^{-1}.

Note that the non-breaking case gives both a higher runup and runup velocity compared to the breaking case where in the latter the waveslope is greater than in the former.

Additional results for the case of deep water will be presented (Grue and Osyka, 2020).

REFERENCES

B. Buchmann, P. Ferrant and J. Skourup, Run-up on a body in waves and current. Fully nonlinear and finite-order calculations. Appl. Ocean Res. 22 (2000) 349-360.

L. De Vos, P. Frigaard and J. De Rouck, Wave run-up on cylindrical and cone shaped foundations for offshore wind turbines. Coastal Engineering 54 (2007) 17-29.

O.M. Faltinsen, M. Landrini and M. Greco, Slamming in marine applications. J. Engng. Math. 48 (2004) 187-217.

J. Grue and B. Osyka, Runup on a vertical column in strong water wave events. Submitted for publication (2020).

T. Lykke Andersen, P. Frigaard, M.L. Damsgaard and L. De Vos, Wave run-up on slender piles in design conditions - Model tests and design rules for offshore wind. Coastal Engineering 58 (2011) 281-289.

J. Zhang and B. Teng, Numerical study on cnoidal wave run-up around a vertical circular cylinder, Appl. Ocean Res. 63 (2017) 276-287 https://doi.org/10.1016/j.apor.2017.01.006